

Screening at a Charged Surface by a Molten Salt

Oliver J. Lanning and Paul A. Madden*

Chemistry Department, Oxford University, South Parks Road, Oxford OX1 3QZ, United Kingdom

Received: May 3, 2004; In Final Form: May 19, 2004

The screening of the electrical potential at a charged solid surface in a molten salt has been investigated in a computer simulation study. The relaxation time associated with the screening is found to be very short, and not dependent on diffusion. Despite pronounced oscillatory structure in the charge density, the structure and dynamics of the ions close to the interface are very similar to those in the bulk.

Introduction

Despite the importance of electrochemical processes in molten salts, there is no well-founded model¹ for the fluid structure and dynamics at an electrified interface comparable to the double-layer description of the electrochemical behavior of electrolyte solutions.² In the absence of an alternative, double-layer ideas are often applied to relate capacitance³ and electrokinetic data to the fluid properties at the atomic scale. However, an early computer simulation study of molten KCl at a charged hard wall, by Heyes and Clarke,⁴ showed a pronounced and relatively long-ranged oscillation of the charge density close to the interface, rather than a double-layer, an observation subsequently confirmed^{5,6} and reproduced in integral equation studies.^{7,8} The development of new types of experiments and the emergence of low-temperature molten salts (or “ionic liquids”) as convenient media for quantitative electrochemical studies have focused attention on the need for a better understanding of the properties of the molten salt in the immediate vicinity of a charged surface.

Grätzel and co-workers⁹ have produced an efficient photo-voltaic device in which the active electrode consists of dye-sensitized TiO₂ nanoparticles suspended in an ionic liquid, which transports charge to the other electrode. He has commented that the ionic liquid plays an important role in maintaining an output current that is linear to high levels of light intensity. It appears that it *rapidly* screens the charge transferred to a nanoparticle, and prevents a coulomb blockade. The molten salt is far more effective than an electrolyte solution of similar conductivity.¹⁰ New reversible square voltametric techniques capable of measuring time-dependent screening phenomena in ionic liquids on the relevant time scale are currently being developed.¹¹

Freyland et al.¹² have reported ellipsometric measurements which bear upon the fluid structure at an electrified interface. They studied the F-center-like spectrum of the electrons which are trapped in a thick ($>100\text{\AA}$) wetting layer of a molten salt at a charged sapphire (Al₂O₃) surface and reported that the absorption band was much narrower than that expected for a molten salt under these conditions. They suggested that the high degree of structuring reported by Heyes and Clarke⁴ suppressed the electrical potential fluctuations close to the surface. Esnouf et al.⁵ had already speculated that the ions within the charged

layers observed in the computer simulations might have a near-crystalline degree of local order.

Methods and Preliminary Results

Molecular dynamics simulations of molten KCl confined between rigid charged walls have been carried out. The calculations are similar to those in the earlier work^{4–6} but larger cells, longer runs, and smaller wall charge densities have been used. The purpose of the calculations is to examine new quantities which bear upon the origins of the phenomena discussed above. Interactions between the ions are described by standard Born–Mayer pair potentials,¹³ with the ions carrying a full electronic charge. The simulation cell, periodically replicated in the x and y directions and confined by charged walls along z , contains 1400 ions in a cell of sides 25.16\AA (x , y) and 107.96\AA in the z direction. This gives an average density similar to that of molten KCl at 1300 K. Each wall consists of 128 fixed particles carrying a fractional charge of magnitude Q (positive for one wall and negative for the other). They were arranged in a 2-D square lattice with a spacing half that of KCl (to give a smooth surface-ion potential). The wall particles experience *short-range* (non-Coulombic) repulsive interactions with the melt ions as if they were K⁺ ions. All Coulombic interactions were computed by using a 2-dimensional Ewald summation due to Kawata and Mikami.¹⁴ The Fortran code was compiled under Linux, using the Intel compiler. A 1000-step run, each step being 1.2 fs, takes ca. 20 min on a 1.66G Hz Intel Zeon processor. On construction of the systems, the melt ions were equilibrated against the walls for 100 000 steps (121 ps). Runs of 500 000 steps (605 ps) were then used to collect the data shown in this paper. The calculations have been performed for a wide range of temperatures and wall charges, but only selected results are described in detail here.

In Figure 1 we show the profiles of the mean total number density ($\rho_{\text{tot}}(z) = \rho_{+}(z) + \rho_{-}(z)$) and the ionic charge density ($\rho_{\text{c}}(z) = \rho_{+}(z) - \rho_{-}(z)$) across the simulation cell for a wall charge density of $3.242\text{ }\mu\text{C cm}^{-2}$ (0.005 electronic charges per wall particle). The total density shows the typical structure of an atomic fluid at a wall,¹⁵ while the charge density shows the oscillatory structure reported by Heyes and Clarke.⁴ The heights of the peaks of the charge density oscillations fall off roughly exponentially with distance from the wall, with a decay length of about 8\AA , which is similar to that of the decay of radial charge correlations in the bulk fluid. This decay constant shows no dependence on the surface charge density, for charges up to

* Address correspondence to this author. E-mail: madden@physchem.ox.ac.uk.

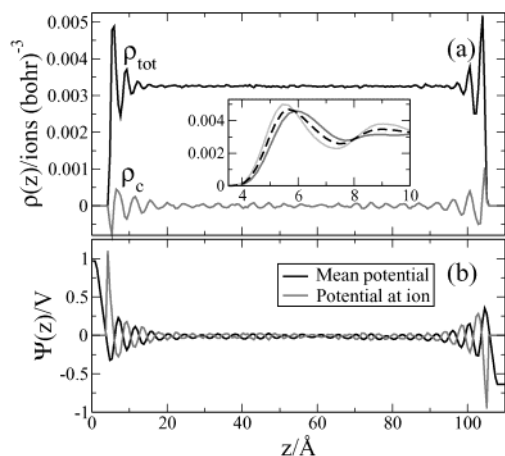


Figure 1. Figure showing density (a) and potential (b) across the cell for a system at a temperature of 1300 K and a wall charge density of $3.242 \mu\text{C cm}^{-2}$. Part a shows the total density, ρ_{tot} , and charge density, ρ_c . The inset contains a detail of the left-hand (positively charged) interface of the cell, showing the total density (dashed black line), the cation density (dark gray), and the anion density (light gray). Both cation and anion densities have been multiplied by a factor of 2 for easy comparison with the total density. Part b shows the mean potential, obtained by spatially integrating Poisson's equation, and the potential at an ion ("Madelung potential"), calculated by dividing the Coulombic potential energy of an ion by its charge.

at least 5 times greater than those illustrated, and only a weak temperature-dependence in the range 1100–1500 K.

At the bottom of Figure 1 we show two measures of the local mean electrical potential. The full line is the total electrical potential (Ψ), obtained by spatially integrating Poisson's equation

$$\nabla^2 \Psi = -\frac{\rho}{\epsilon_0} \quad (1)$$

with the average charge density (including the wall charges) as the source. The other curve shows the "Madelung potential", which is the average of the potential experienced by an ion at position z , and therefore governs the fluid structure and dynamics. The Madelung potential excludes the contribution of that ion's charge to the local potential, and therefore differs from the total potential by a term roughly proportional to the local charge density. For KCl, where the cation and anion are of similar size, the Madelung potentials for both ions are quite similar. Away from the walls the potential is constant, indicating that the molten salt completely screens the wall charge within about 20 \AA from the surface. In the vicinity of the walls the potential oscillates rapidly, which is qualitatively inconsistent with a double-layer description of the interface. Note, however, that the potential drops to a low value *very* close to the surface (within the first layer of the total density). Consequently, in an electrochemical system, an ion that could be oxidized at a high potential would still have to access the region very close to the surface and the (diffusive) kinetics of this process might therefore still resemble those expected from conventional (double-layer) electrokinetics with a very short screening length.

A comparison between the properties of the simulated system and a real electrochemical interface must be treated with care, especially when the solid surface is metallic. As Figure 1 shows, there is a very large electric field across the interface. This field would be screened by the conduction electrons of the metal, giving the electric potential a very different profile across the region between the first layers of the ions in the surface and

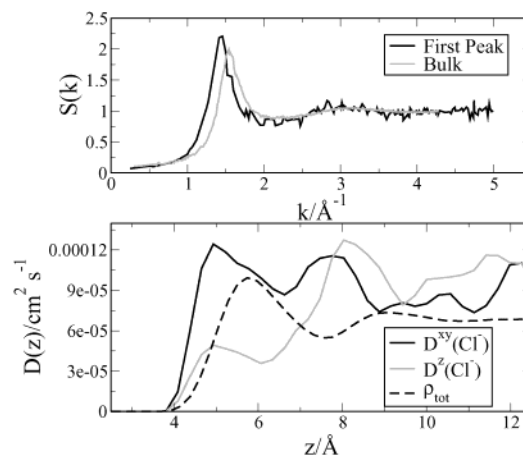


Figure 2. The top panel of the figure shows the comparison of the anion–anion partial structure factors for the first density peak against the positively charged (left-hand) wall of a system at a wall charge density of $32.42 \mu\text{C cm}^{-2}$ and 1300 K. This is compared to the anion–anion partial structure factor peak of a bulk system at 1300 K and the same density. The lower panel of the figure shows the Cl^- ion diffusivities both parallel and normal to the interface as a function of the z position of the ion at the start of diffusion. The density profile, $\rho_{\text{tot}}(z)$, is included for comparison (dashed line).

the melt, as has been emphasized in *ab initio* treatments of the metal–aqueous electrolyte interface.¹⁶ Furthermore, we have neglected the polarization of the surface by the ions (image charges), the polarization of the ions, and also located the wall charges at the centers of the wall particles, which will also affect the electric potential.¹⁷ We are currently extending our calculations to examine the effect of the latter three simplifications. Ultimately, we might hope to be able to compare a realistic model for the interface with results on the structure and dynamics obtained from experiments of the type now performed at the air/water interface.¹⁸ For the present, we may calculate a capacitance (C) for the interface from the drop in potential ($\Delta\Psi$) between the wall ($z = 0$) and the center of the cell and the surface charge density σ

$$C = \frac{\sigma}{\Delta\Psi} \quad (2)$$

For the cell illustrated in Figure 1, the potential drop is $\sim 1 \text{ V}$, which gives a capacitance of $3.191 \mu\text{F cm}^{-2}$. Kiszka³ has recently reported a "double-layer" capacitance of $2.91 \mu\text{F cm}^{-2}$ for KCl at an ideally polarizable Mg electrode: in view of the above reservations, this good agreement must be at least partially fortuitous.

As the inset to Figure 1 (which highlights the left-hand, positively charged interface) shows, the charge density oscillations *do not* correspond to alternating layers of positive and negative ions at this (experimentally relevant) level of the interfacial potential. Instead each peak of the total density is polarized, with a slight excess of negative ions toward the wall. At much higher values of the surface charge density ($\sim 32 \mu\text{C cm}^{-2}$), the character of the interface does change, and discrete layers of positive and negative ions, which correspond to maxima in the total charge density, are formed.

Structure and Dynamics of the Screening Layer

In Figure 2 we illustrate the extent to which the properties of the ions close to the surface differ from those in the bulk. The upper panel shows the in-plane anion–anion structure factor

for a layer of ions; it corresponds to a diffraction experiment with scattering vector \mathbf{k} lying in the xy plane of the interface

$$S(k, z) = \langle A(\mathbf{k}, z) A^*(\mathbf{k}, z) \rangle \quad (3)$$

The scattering amplitude for the anions in a layer at position z is given by

$$A(\mathbf{k}, z) = N^{-1/2} \sum_{i \in z} e^{i\mathbf{k} \cdot \mathbf{r}_i} \quad (4)$$

where \mathbf{r}_i is the position of ion i and the sum is over all anions within the layer at z . In the figure, we contrast the structure factor for the layer which contains the first peak in the total density against the interface (Figure 1) with that for the bulk. Except for a small shift of the peak to lower k , the structure of the first layer is remarkably similar to the bulk: in particular, there is no suggestion of quasicrystalline ordering.

The lower panel of Figure 2 shows the behavior of the local diffusion coefficients of the ions (again, close to the positively charged surface). The quantity

$$D_i^\alpha(t) = \frac{1}{2\Delta t} [\mathbf{r}_{\alpha,i}(t + \Delta t) - \mathbf{r}_{\alpha,i}(t)]^2 \quad (5)$$

is averaged over all ions which at time t are found within a layer centered at position z , and then averaged over initial times, to give an estimate of the diffusion coefficient along the direction α for those ions initially within that layer. The interval Δt was taken to be 0.5 ps—short enough to ensure that the *local* mobility is being sampled. The figure shows that the in-plane mobility of the anions close to the surface is remarkably similar to the bulk, again ruling out quasicrystalline ordering. The diffusion perpendicular to the interface of the anions in the first layer is slowed compared to that of the bulk. In part, this is simply because these ions cannot penetrate the wall and can only undergo displacements to positive z , and there is no suggestion that the ions adhere to the wall through Coulombic interactions with the wall charges.

According to Siringo and Logan,¹⁹ the width of an absorption band associated with electrons localized at some site is proportional to the root-mean-square value of the fluctuations in the Madelung potential at that site. We may therefore examine Freyland et al.'s suggestion,¹² that the narrowness of the absorption spectrum associated with the excess electrons in a KCl wetting layer is due to the charge-ordering phenomenon illustrated in Figure 1, by calculating the mean-square fluctuation in the Madelung potential as a function of distance from the surface. The results are illustrated in Figure 3 for a wall charge density of $3.242 \mu\text{F cm}^{-2}$ and a temperature of 1300 K: the mean Madelung potential (as in Figure 1) is also shown. They indicate that there is a suppression of the Madelung potential fluctuations with respect to the bulk, but only in a region very close to the wall—within the first maximum of the peak in the total number density. To account for the experimental data straightforwardly, it would be necessary for this effect to extend much further into the fluid—comparable to the penetration depth of the evanescent wave of light reflected at the charged surface. It would appear that some other explanation of the narrowness of the F-center band in the wetting layer at the sapphire surface is required.

The relaxation of the screened electrical potential following a change in the value of the surface charge may be examined, at $t = 0$, by reversing the sign of the charges on the wall ions and following the potential across the cell at subsequent times. In practice, we have examined the Madelung potential on the

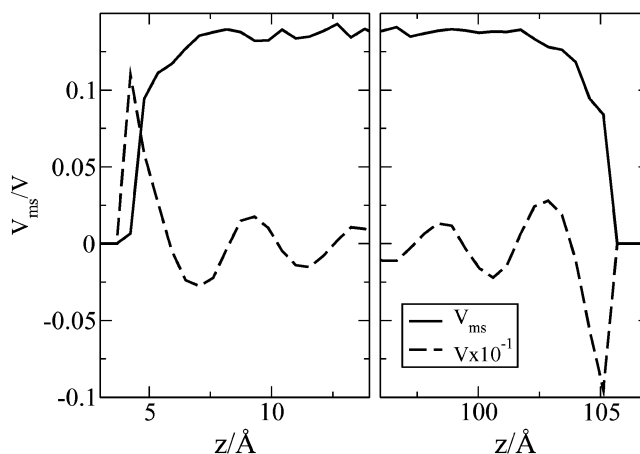


Figure 3. Figure showing the mean-square fluctuations of the potential, $V_{\text{ms}} = \langle V^2 \rangle - \langle V \rangle^2$, as a function of z position of the ion, from a system with a wall charge density of $3.242 \mu\text{C cm}^{-2}$ at 1300 K. Also shown with a dashed line is the actual potential, scaled by a factor of 0.1 for comparison.

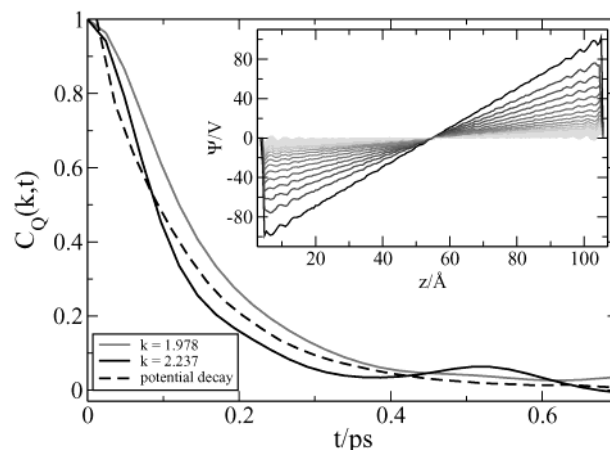


Figure 4. The relaxation of the electrical potential following a change in the value of the wall charges at $t = 0$. The inset shows the profiles of the Madelung potential across the cell for successive intervals of time of length 2.4×10^{-2} ps after this initial change. They are plotted black to light gray with 30 lines in total. In the main figure the value of this potential at some reference position within the cell is plotted versus delay time (dashed line). Also shown are the charge-density correlation functions (see text) for $k = 1.978$ and 2.237 Å^{-1} with which this transient is to be compared.

melt ions within spatial bins of width 0.56 Å and temporal bins of duration 0.024 ps over 30 transients. The results are illustrated in the inset to Figure 4. Immediately after the charges are reversed, there is a large potential gradient across the cell due to the surface charge and also the screening density, which had built up for $t < 0$, when the cell had the opposite polarity. This potential relaxes away in a uniform manner as the polarization of the screening layer adapts to the change in the wall charges. The decay transient at a point within the cell, averaged over values taken between $z = 20\text{--}40$ and $70\text{--}90 \text{ Å}$, is shown in the main body of the figure. It indicates a remarkably rapid relaxation of the screening layer, consistent with Grätzel's comment,^{9,10} that the screening relaxes much more rapidly in a molten salt than an electrolyte solution. The decay constant is about 0.14 ps : it is found to be independent of the wall charge up to $\sim 20 \mu\text{C cm}^{-2}$ and only weakly dependent on temperature. Were the screening to be due to an excess of ions of opposite charge to the wall ions contained within some double layer, as in an electrolyte solution, we might estimate a relaxation time of order $l^2/2D$, where l is the width of the screening layer (~ 20

Å, from Figure 1) and D the diffusion coefficient ($\sim 1.4 \times 10^{-4} \text{ cm}^2 \text{ s}^{-1}$ at 1300 K). This gives a time that is 3 orders of magnitude longer than that observed.

In reality, the nature of the screening in the molten salt is, as illustrated in the inset to Figure 1, due to a local polarization of the high density layers at the surface. This can relax very rapidly because it only requires very small distance movements of individual ions (in the inset to Figure 1, the distance between the maxima of the positive and negative charge densities is only ~ 1 Å). Furthermore, because the melt is locally polarized, unless the charge densities are equal, this motion is driven by a local electric field. A more reasonable comparison is with the relaxation time of a Fourier component of the charge density of the bulk fluid,²⁰

$$C_Q(k, t) = \left\langle \sum_i q_i \exp(i\mathbf{k} \cdot \mathbf{r}_i(t)) \sum_j q_j \exp(-i\mathbf{k} \cdot \mathbf{r}_j(0)) \right\rangle \quad (6)$$

calculated at a wavevector \mathbf{k} whose magnitude corresponds to the period of the oscillations in the charge density at the interface (Figure 1). This value is about 2.1 Å^{-1} , and in Figure 4 we have included results for $C_Q(k, t)$ with $k = 1.978$ and 2.237 Å^{-1} calculated from a bulk simulation at the same temperature and density to compare with the observed transient. Given that the transient is obtained by an average over temporal bins of width 0.024 ps (which affects the shape of the transient at small times), the agreement is good. The theory of the relaxation of the charge density in a simple molten salt is described in ref 20. At these high wavevectors (compare the structure factor in Figure 2), the charge density is relaxed by small scale translations of the ions and coupled to the local electric field, which generates very rapid relaxation. Because of the short length scale and the drive to local charge neutrality, the relaxation is not coupled to diffusive processes and hence the relaxation time is only weakly temperature dependent compared to the diffusion coefficient. It should remain rapid in any coulomb fluid—even one which is more viscous than molten KCl—like most low-temperature molten salts.

Summary

We have examined the structure and dynamics of the liquid close to a charged interface to examine issues suggested by recent experiments. At physically reasonable values of the surface charge density, these properties are very similar to those in the bulk fluid, despite the presence of well-defined oscillations in the mean number and charge densities. Nevertheless, we have shown that the molten salt responds extremely rapidly to changes in the surface charge density, and rapidly screens the potential due to the surface charge. We have used a particularly simple model for the molten salt, and also for the charged solid surface. However, we would expect the findings to apply generally in fully dissociated ionic liquids—even when the ions comprise the large organic entities present in low-temperature molten salts.

References and Notes

- (1) Parsons, R. *Chem. Rev.* **1990**, 90, 813.
- (2) Bockris, J. O'M.; Reddy, A. K. N. *Modern Electrochemistry*; Plenum/Rosetta: New York, 1977.
- (3) Kiszka, A. *J. Electroanal. Chem.* **2002**, 534, 99.
- (4) Heyes, D. M.; Clarke, J. H. R. *J. Chem. Soc., Faraday Trans. 2* **1981**, 77, 1089.
- (5) Esnouf, R. M.; Smith, A. C. D.; Grout, P. J. *Philos. Mag. A* **1988**, 58, 27.
- (6) Boda, D.; Henderson, D.; Chan, K.-Y. *J. Chem. Phys.* **1999**, 110, 5346.
- (7) Booth, M. J.; Haymet, A. D. J. *Mol. Phys.* **2001**, 99, 1817.
- (8) Li, S.; Mazo, R. M. *J. Chem. Phys.* **1987**, 86, 5757.
- (9) Grätzel, M. *Nature* **2001**, 414, 338. Grätzel, M. *Nature* **2003**, 421, 586.
- (10) Grätzel, M. Private communication.
- (11) Oldham, K. B.; Gavaghan, D. J.; Bond, A. M. *J. Phys. Chem. B* **2002**, 106, 152.
- (12) Tostmann, H.; Nattland, D.; Freyland, W. *J. Chem. Phys.* **1996**, 104, 8777.
- (13) Fumi, F. G.; Tosi, M. P. *J. Phys. Chem. Solids* **1964**, 25, 31. Fumi, F. G.; Tosi, M. P. *J. Phys. Chem. Solids* **1964**, 25, 45.
- (14) Kawata, M.; Mikami, M. *Chem. Phys. Lett.* **2001**, 340, 157.
- (15) Evans, R.; Leote de Carvalho, R. J. F.; Henderson, J. R.; Hoyle, D. C. *J. Chem. Phys.* **1994**, 100, 591.
- (16) Walbran, S.; Mazzolo, A.; Halley, J. W.; Price, D. L. *J. Chem. Phys.* **1998**, 109, 8076.
- (17) Schmickler, W. *Chem. Rev.* **1996**, 96, 1996.
- (18) Benderskii, A. V.; Eissenthal, K. B. *J. Phys. Chem.* **2002**, 106, 7482.
- (19) Logan, D. E.; Siringo, F. *J. Phys.: Condens. Matter* **1992**, 4, 3695.
- (20) Hansen, J. P.; McDonald, I. R. *Theory of Simple Liquids*; Academic Press: New York, 1976.